

The BES $f_0(1810)$: a new glueball candidate

P. Bicudo¹, S.R. Cotanch², F.J. Llanes-Estrada^{3,a}, D.G. Robertson⁴

¹ Departamento de Física and CFTP, Instituto Superior Tecnico, 1049-001 Lisboa, Portugal

² Department of Physics, North Carolina State University, Raleigh, NC 27695, USA

³ Departamento de Física Teórica I, Universidad Complutense de Madrid, 28040 Madrid, Spain

⁴ Department of Physics and Astronomy, Otterbein College, Westerville, OH 43081, USA

Received: 29 March 2007 / Revised version: 1 July 2007 /

Published online: 11 August 2007 – © Springer-Verlag / Società Italiana di Fisica 2007

Abstract. We analyze the $f_0(1810)$ state recently observed by the BES collaboration via radiative J/ψ decay to a resonant $\phi\omega$ spectrum and confront it with DM2 data and glueball theory. The DM2 group only measured $\omega\omega$ decays and reported a pseudoscalar but no scalar resonance in this mass region. A rescattering mechanism from the open flavored $K\bar{K}$ decay channel is considered to explain why the resonance is only seen in the flavor asymmetric $\omega\phi$ branch along with a discussion of positive C -parity charmonia decays to strengthen the case for preferred open flavor glueball decays. We also calculate the total decay width of a glueball with this mass to be roughly 100 MeV, in agreement with the narrow, newly found f_0 , and smaller than the expected estimate of 200–400 MeV. We conclude that this discovered scalar hadron deserves further experimental investigation, especially in the $K\bar{K}$ channel, and if shown to be different from the $f_0(1710)$, will become a solid glueball candidate. Finally we comment on other, but less likely, possible assignments for this state.

1 Introduction

Significant in the recent wave of particle discovery, the BES collaboration has reported [1] a scalar hadron with mass about 1812 MeV and width of $105(20)$ MeV. This $f_0(1810)$ state appeared as a 95 event enhancement in the $\omega\phi$ spectrum accompanied by a radiative photon from 5.8×10^7 J/ψ decays. This paper considers several interpretations for this state and focuses on the most exciting assignment, the long-sought scalar glueball.

Past speculation on the glueball mass encompassed values between 500 MeV and 2 GeV. More currently, the mass region below the $f_0(980)$ is excluded by the leading N_c analysis of chiral perturbation theory and a firmer Sigma meson [2] assignment. Moreover, the pomeron–glueball connection [3, 4] implies that the tensor 2^{++} glueball is in the mass region of 2.2–2.4 GeV, and no reasonable model that correctly describes conventional vector mesons can accommodate a scalar glueball below, say, about 1.4 GeV, with 1.8 GeV being favored. Some lattice and many body calculations seem in agreement with this phenomenological observations and predict glueball masses well above 1 GeV, see respectively [5] and [4, 6], with both approaches agreeing that the ground state has quantum numbers 0^{++} and lies in the range 1700 to 1800 MeV. One should however take note of competing lattice calculations that predict 1600 MeV [7], and 1550 MeV [8]. Thus it would appear that contemporary computations of the glueball

mass are consistent with the new BES state, without discarding nearby and lower mass candidates.

Scalar hadrons between 1 and 2 GeV, predominantly the $f_0(1370)$, $f_0(1500)$ and $f_0(1710)$, have been scrutinized for glueball wavefunction components in numerous studies [9–12]; however, firmly identifying gluonic degrees of freedom remains elusive [13]. In this paper we dispel several theoretical conjectures about the scalar glueball and show that the discovered BES state is a good glueball candidate, meriting more careful study. Using a QCD-based model we calculate that the full glueball decay width is about 100 MeV, which is consistent with the measured 105 ± 20 MeV width for the $f_0(1810)$. We also show that the commonly assumed flavor blind glueball decay treatment entails large corrections, yielding a measurable $\omega\phi$ branch but a suppressed $\omega\omega$ channel, again consistent with new data. This has also been pointed out recently by Chanowitz [14]. Finally we demonstrate how the rescattering mechanism, $f_0(1810) \rightarrow K\bar{K} \rightarrow \phi\omega$, facilitates observing $\phi\omega$ cleanly above the tail of the predominant $f_0(1710) \rightarrow K\bar{K}$ spectrum, given sufficient precision.

2 Phenomenological considerations

2.1 Contrasting BES with DM2 and Mark III data

About two decades ago the DM2 collaboration observed at Orsay 8.6×10^6 J/ψ decays and studied the $\omega\omega$ spec-

^a e-mail: fllanes@fis.ucm.es

trum triggered by radiative decay (photon decays have a 1% branch due to $\alpha_{\text{EM}}/\alpha_s$ suppression). They reported [15] a branching ratio, $B(J/\psi \rightarrow \gamma\omega\omega) = 1.4(0.2)(0.4) \times 10^{-3}$, much larger than the BES $\gamma\omega\phi$ ratio, $B(J/\psi \rightarrow \gamma\omega\phi) = 2.61(0.27)(0.65) \times 10^{-4}$, and observed a strong pseudoscalar $\eta(1760)$ enhancement but concluded that there was no relevant structure near or above 1800 MeV. Of course the $\omega\omega$ decay must correlate with about $3\rho\rho$ decays and indeed [16] observed a similar pseudoscalar signal in $\rho\rho$ about 100 MeV wide, but threshold effects make it difficult to compare these two experiments. A related issue is that there should also be a correlation with the $\omega\phi$ channel [17, 18] (note that DM2 was not designed to detect $\omega\phi$); however, this can only be observed for resonances above the $\omega\phi$ 1802 MeV threshold (it would also be kinematically suppressed unless significantly above threshold).

Most recently, the BES collaboration also reported [19] an analysis of $J/\psi \rightarrow \gamma\omega\omega$ from the same $5.8 \times 10^7 J/\psi$ BESII detector data set. They clearly confirm the $\eta(1760)$ (mass 1744 MeV, width 244 MeV) and also evidence for a 0^{++} structure, which could correspond to the $f_0(1710)$ and/or $f_0(1810)$. However, it is difficult to determine the mass and width of this scalar hadron due to the dominant contributions from the $\eta(1760)$.

We submit that the absence of the $f_0(1810)$ scalar resonance, independent of its quark-gluon structure, in the DM2 and BESII $\omega\omega$ spectra indicates that the $f_0(1810)$ decay is not flavor blind. This is because the BESII $\omega\phi$ signal, combined with flavor independent decay (omitting phase space effects), predicts an $\omega\omega$ signature that would have also been observed by BESII and DM2. To quantify this, we compute the ratio, R , of $\omega\omega$ to $\omega\phi$ phase space factors, $P(m)$, folded with a Breit–Wigner

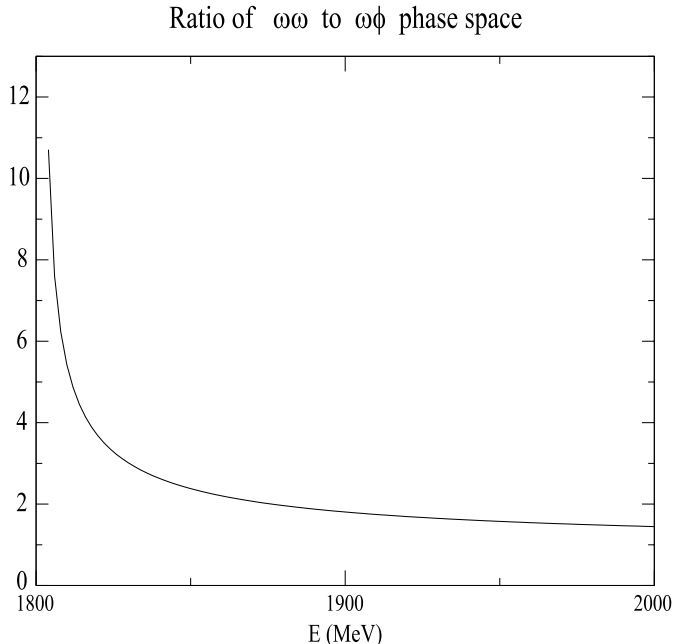


Fig. 1. Ratio of $\omega\omega$ to $\omega\phi$ for a Breit–Wigner folded with phase space

Table 1. $\omega\omega$ events that DM2 would have observed in the 0^{++} channel assuming flavor blind decay. Only four events were recorded by DM2, indicating a preference for open flavor decay. Units for Γ and M_{f_0} are GeV

M_{f_0}	Γ	R	Predicted DM2 events
1.812	0.105	3.9	56
	0.085	4.1	
	0.125	3.8	
1.793	0.103	5.0	71
1.838	0.105	3.0	43

profile (see Fig. 1),

$$R = \frac{\int_{\omega\omega\text{th}}^{2 \text{ GeV}} dm \frac{P_{\omega\omega}(m)}{(m-M_{f_0})^2 + \Gamma_{f_0}^2/4}}{\int_{\omega\phi\text{th}}^{2 \text{ GeV}} dm \frac{P_{\omega\phi}(m)}{(m-M_{f_0})^2 + \Gamma_{f_0}^2/4}}. \quad (1)$$

Multiplying R by the number of BES $f_0(1810)$ observed events (95) and the ratio of DM2 to BES J/ψ total decays ($8.6 \times 10^6 / 5.8 \times 10^7$) yields 58 $f_0 \rightarrow \omega\omega$ events DM2 would have reported, assuming equal reconstruction efficiencies and a $f_0(1810)$ flavor blind decay. However, as detailed in Fig. 2, DM2 only reported 4 $\omega\omega$ events in the 0^{++} channel, which undermines the $f_0(1810)$ flavor blind decay assumption. Predictions for other possible f_0 mass assignments are summarized in Table 1. Also, rescaling the BES data sample size for appropriate comparison (see

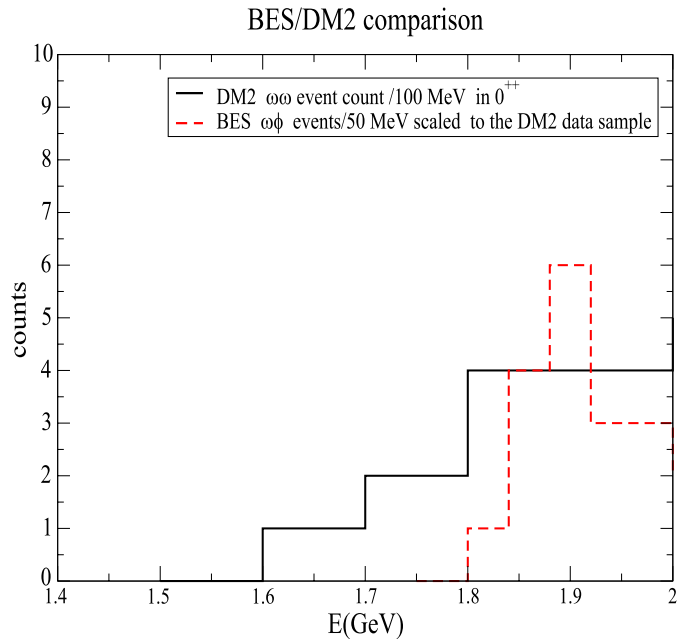


Fig. 2. Dashed line: BES $\omega\phi$ events rescaled to the DM2 sample size. Solid line: actual $0^{++}\omega\omega$ DM2 measurement. A DM2 confirming an $\omega\phi$ decay signal is not possible due to the small J/ψ sample used

dashed line in Fig. 2), yields at best only a few (less than 4) $\omega\phi$ events that the DM2 collaboration would be expected to observe. It would appear that the number of events in the DM2 J/ψ sample is insufficient to determine whether a resonance is or is not present in their $\omega\phi$ spectrum even if they were looking for it.

The DM2 data are in overall agreement with the Mark III data at SLAC (see [20] and references therein). The Mark III $K\bar{K}$ and $\pi\pi$ spectra featured a prominent $f_0(1710)$ but no $f_0(1810)$ state. Somewhat perplexing, BES reported a low statistics study of the $K^*\bar{K}^*$ spectrum in radiative J/ψ decays [21] with the 0^{++} channel not significantly populated. We also note that the more recent 294 $\gamma\omega\phi$ events cleanly isolated by BES, although only part of the total produced, represent an extremely small branching fraction compared to, for example, $B(J/\psi \rightarrow \gamma K^*\bar{K}^*) = 4(1) \times 10^{-3}$.

The $f_0(1810)$ decay profile is perplexing. While suppressed rates to the $K^*\bar{K}^*$ channel can be understood (note that conservation of J^P forbids decay to $K^*\bar{K}$ and $\rho\pi$) due to limited phase space (see next section), what scalar hadron would decay leaving a clear signal in $\omega\phi$ but apparently none in either of $K\bar{K}$, $\pi\pi$ or, most significantly, $\rho\rho$ and $\omega\omega$? In the next section we explain the suppressed $\rho\rho$ and $\omega\omega$ decays by arguing that open flavor (strangeness) glueball decays are favored and that $K\bar{K}$ rescattering plays an important role in the $\omega\phi$ final state.

2.2 Radiative charmonium decay and glueball formation

Consider the radiative J/ψ decay to a $C = +1$ charmonium (on or off-shell) that subsequently decays. Having positive C -parity favors decay via intermediate two gluon states and the resulting spectra should therefore display resonances corresponding to the glueball masses. A simple diagrammatic analysis (see Fig. 3) reveals that open (explicit) flavor decays, which we call “fall apart”, dominate over closed (hidden) flavor decays that require color exchange. Here the time axis is horizontal and the (on- or off-shell) decay sequence is: a charmed hybrid, glueball, light hybrid and finally a tetraquark system. This yields

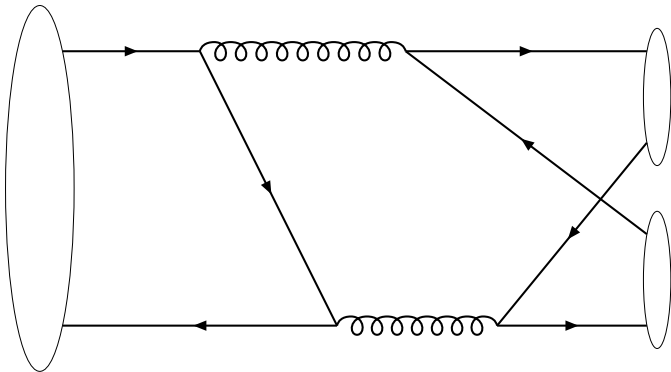


Fig. 3. Depiction of a $C = +$ charmonium decay via gluonic and quark intermediate time steps (other orderings are possible)

Table 2. Selected $C = +1$ charmonium branching fractions with explicit and hidden strangeness. All numbers should be multiplied by 10^{-3}

Channel	$0^{-+}(\eta_c)$	$0^{++}(\chi_c^0)$	$1^{++}(\chi_c^1)$	$2^{++}(\chi_c^2)$
$K^*\bar{K}^*$	9(3)	4(1) [†]	6(2) [†]	8(2) [†]
$K^+K^-\pi^+\pi^-$	15(6)	20(4)	4.5(10)	10(2)
$K^+\bar{K}^{*0}\pi^- + cc$	20(7)	12(4)	3(2)	5(3)
$\omega\omega$	< 3	2.3(7)		2(1)
$\phi\phi$	2.7(9)	0.9(5)		2(1)
$K^+K^+K^-K^-$		2.1(3)	0.39(17)	1.4(3)

[†]assuming isospin symmetry

a preference for open flavor mesons (e.g. pseudoscalar or vector kaons) over closed (hidden) flavor $\omega\phi$ that requires final state rescattering. Table 2 further supports this point, listing established $C = +1$ charmonia decays [22] to predominantly open flavor meson states. The data are best interpreted by assuming a “fall-apart” decay mechanism with open flavor dominating over the closed strangeness decay that requires color exchange (rescattering). In addition to the $\phi\phi$ decay we enter the four kaon decay. Likewise in addition to the $K^*\bar{K}^*$ ratio we listed the branching fraction to two charged pions and two charged kaons. Both sets of numbers seem consistent. Note that the argument of preferential open flavor decay and our invocation of charmonium decays does not depend on the J^P quantum numbers of the state, being only tied to the positive C -parity.

3 Glueball decay widths

3.1 Existing estimates

In previous work we and others have published estimates for glueball widths which we now summarize before presenting new computations. First, there is the lattice estimate [23] of about 100 MeV. That calculation proceeds by computing the glueball-to-two meson couplings on the lattice, with the help of simple linear extrapolation in the meson mass, and then using the coefficients as the coupling vertices of an effective decay Lagrangian density from which the two-body width follows.

As detailed in [17, 18] the width for the decay of a scalar glueball G to two vector mesons, $G \rightarrow VV'$, is

$$\Gamma_{G \rightarrow VV'} = \frac{g_{G V V'}^2}{4\pi} \frac{k^3}{M^2}, \quad (2)$$

where $M = 1$ GeV is a fixed reference mass, $g_{G V V'}$ is the $G V V'$ coupling constant and k is the CM momentum for the decay vector mesons, given by $k = (M_G/2)[(1 + x - x')^2 - 4x]^{1/2}$, with $x = (M_V/M_G)^2$, $x' = (M_{V'}/M_G)^2$ and M_G the scalar glueball mass (now tested against 1812 MeV). Using vector meson dominance (VMD), [18] obtained $g_{G V V'} = 4.65$, which gives a small partial width of 1.43 MeV for the $\omega\phi$ decay, reflecting the near threshold suppressed phase space. An independent work [24, 25] reports a similar value for the coupling, $g_{G V V'} = 4.23$.

Table 3. Partial widths (in MeV) for various values of the glueball mass and coupling. N/P indicates insufficient phase space. The final column is the sum of the other columns and represents a lower bound for the total width

M_{f_0}	$g_{GVV'}$	$\Gamma_{\omega\phi}$	$\Gamma_{\rho\rho}$	$\Gamma_{\omega\omega}$	$\Gamma_{K^*K^*}$	Γ_{tot}
1700	4.65	N/P	72.1	62.8	N/P	135
1812		1.43	176	164	4.10	346
1831		7.16	198	184	11.3	401
1700	4.23	N/P	59.7	52.0	N/P	112
1812		1.18	146	135	3.39	286
1831		5.92	164	153	9.38	331

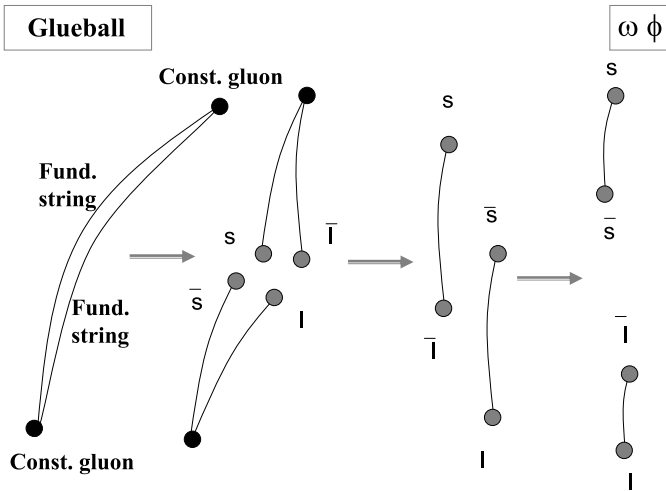


Fig. 4. Illustrating glueball decay with final state rescattering of the produced kaons to yield $\omega\phi$

If we assign the larger glueball mass $M_G = 1812 + 19 = 1831$ MeV, using the BES quoted upper statistical error, the $\omega\phi$ partial width increases to 7.16 MeV. For the maximum possible mass (including the quoted 18 MeV systematic error) of 1849 MeV the width further increases to 15 MeV. Table 3 lists predictions for other two-body decays along with parameter sensitivity. Relying on these results alone would suggest that the glueball width is much broader than the $f_0(1810)$ BES candidate and its decay branching fraction to $\phi\omega$ is insignificant.

Another glueball approach [26], based upon a string model, predicts a different, smaller total width, $\Gamma_G = 140$ MeV. The decay mechanism (with inelastic rescattering of the kaons in the final state) in this constituent model is illustrated in Fig. 4. Their total width is much narrower than expected from VMD but more comparable to the width of the BES candidate. In view of this disagreement between simple string and VMD estimates we have performed a new, first-principles calculation of the glueball width, which is described in the next section.

3.2 Ab-initio glueball width computation

A more fundamental, QCD-based calculation, but independent from lattice gauge theory, for the total width can

be obtained using many body theory [27]. In this relativistic, field theoretical approach an effective Coulomb gauge QCD Hamiltonian is approximately diagonalized using the BCS and TDA many body treatments for the vacuum (gap equation with dressed gluons) and hadron states, respectively. The results are briefly described, with further details relegated to Appendix A.

The glueball is represented by the lightest Fock state consisting of two constituent BCS transverse gluons, which decay to two quark pairs that subsequently hadronize. The decay matrix element is

$$\mathcal{M} = \langle G | \frac{1}{2} \int d\mathbf{x} d\mathbf{y} \mathcal{H}_{qg}(\mathbf{x}) g(\mathbf{x}, \mathbf{y}) \mathcal{H}_{qg}(\mathbf{y}) | qq\bar{q}\bar{q} \rangle, \quad (3)$$

where the quark–gluon Hamiltonian field interaction density is specified in the Appendix A and $g(\mathbf{x}, \mathbf{y})$ is the propagator for intermediate scalar hybrid meson states. The scalar glueball state involving BCS quasi-gluon creation operators $\alpha^{\dagger a}$, with color index a , operating on the BCS vacuum $|\Omega\rangle$, is

$$|G\rangle = \int \frac{d\mathbf{k}}{(2\pi)^3} \frac{\phi(\mathbf{k})}{\sqrt{4\pi}} \frac{\sqrt{M_G}}{4} \alpha^{\dagger a}(\mathbf{k}) \cdot \alpha^{\dagger a}(-\mathbf{k}) |\Omega\rangle, \quad (4)$$

with wavefunction normalization

$$\int \frac{d\mathbf{k}}{(2\pi)^3} \frac{|\phi(\mathbf{k})|^2}{4\pi} = 1. \quad (5)$$

The unit normalized quark state is

$$|q\lambda\rangle = \sqrt{2E} \sum_{c=1}^3 B_{\lambda c}^{\dagger}(\mathbf{q}) \hat{e}_c |\Omega\rangle, \quad (6)$$

for dressed quark creation operator $B_{\lambda c}^{\dagger}(\mathbf{q})$ and color vector \hat{e}_c . Finally, the width is given by

$$d\Gamma = \frac{1}{2M_G} |\mathcal{M}|^2 d\Phi_4, \quad (7)$$

where the four-body phase space for the final quarks is

$$d\Phi_4 = (2\pi)^4 \delta^4 \left(M_G - \sum_{i=1}^4 E_i \right) \left(\prod_{i=1}^3 \frac{d\mathbf{q}_i}{(2\pi)^3 2E_i} \right) \frac{1}{2E_4}. \quad (8)$$

Consult Appendix A for the remaining, technical details of this large-scale, multidimensional integral calculation. However, using dimensional analysis immediately reveals that the total width is of order 100 MeV. Numerical predictions are listed in Table 4. The first column is our reference calculation and lists the widths for a glueball with mass 1812 MeV and a flavor independent quark–gluon coupling vertex. The second column is for a flavor dependent and stronger sgg vertex, inspired by a Landau gauge study in which resummed, leading N_c radiative corrections were more suppressed for light quarks. The dependence on flavor factors follows directly from (A.17). The third column illustrates the sensitivity to the glueball wavefunction. The calculation is the same as the first column, except that the TDA wavefunction is taken from [4], where

Table 4. Total and partial widths for a scalar glueball with mass 1812 MeV. ‘Light’ refers to a light u/d quark–antiquark pair and ‘strange’ denotes a $s\bar{s}$ pair

Widths (MeV)	Flavor independent qqg vertex	$ssg \simeq \frac{10}{7}uug(ddg)$	G wf. from [4], $\Lambda = 8$ GeV	G wf. from [4], $\Lambda = 0.9$ GeV
Γ_{tot}	100	175	50	90
$\Gamma_{\text{light-light}}$	50	50	25	45
$\Gamma_{\text{light-strange}}$	30	65	15	30
$\Gamma_{\text{strange-strange}}$	15	60	5	10

a slightly lighter scalar glueball mass of about 1725 MeV was calculated (however we maintain the BES 1812 MeV kinematics/phase space). Finally the fourth column illustrates the sensitivity to the momentum cut-off used in the calculation and represents probability flux leaking to other channels. Wavefunction components leading to total momentum/energy above the mass of the decaying glueball are virtual and suppress the width. Eliminating them by artificially reducing the cut-off in the glueball wavefunction to $M_G/2$ increases the width by about a factor of 2, which is also the upper bound to the cut-off sensitivity.

Note that in contrast to the above phenomenological models, the calculated total widths from the more fundamental theory are narrower, of order 100 MeV, and consistent with the BES measurement. Indeed, our result also affirms an argument for narrow glueball widths published [28] some time ago based on the OZI rule and originally applied to the oddball (three gluon 1^{--} glueball [27]). The assertion was that charmonia decay dominantly via a glueball/oddball intermediate state, which in turn selects light hadron decay channels, so that the actual width of the glueball is about the geometric mean of the width of OZI-allowed and OZI-suppressed decays, of order of a few tens of MeV.

Concluding this subsection, our best estimate for the total glueball width is about 100 MeV. This estimate is based on a field theory approach where conventional mesons and glueballs are treated simultaneously and with the same parameters, as opposed to phenomenological hadron models or exclusively constituent glueball models (that also have problems of their own). It is noteworthy that the estimate is in agreement with existing lattice computations, although neither should be expected to be more accurate than roughly a factor of 2. Of course, this field theory approach also predicts the mixing between these different Fock space sectors, and we argue in Appendix B.4 below that this mixing will not substantially alter the width of the largely-glueball state. More detailed estimates are planned for the near future.

3.3 Width ratios including final state rescattering

We have also evaluated final state effects and present further details in Appendix B. Here we qualitatively comment and focus on a simple rearrangement potential between the $K\bar{K}$ and $\phi\omega$ channels. This flavor exchange, contact potential couples different channels and illustrates how the $\omega\phi$

signal can arise from other channels by final state rescattering. Table 5 lists the ratio of channel 2 to 1 partial widths for different potential strengths.

The widths are calculated using second order perturbation theory, which should be reasonable as long as the width ratio remains below 1. Also note that $K^*\bar{K}^*$ and $\rho\rho$ rescattering effects are suppressed by their large widths (50 and 150 MeV, respectively), which will broaden any signal and are thus not relevant to the narrow BES state. More promising is the $K\bar{K} \rightarrow \omega\phi$ rescattering process, which is somewhat smaller but still sizeable.

Other factors explain why the $\pi\pi \rightarrow \omega\omega$ process is not important. Whereas the two processes

$$\begin{aligned} G &\rightarrow K\bar{K} \rightarrow \omega\phi, \\ G &\rightarrow \pi\pi \rightarrow \omega\omega \end{aligned}$$

have similar rescattering strengths, there is a factor of about 2 suppression with respect to the $\omega\phi$ due to the stronger strange quark coupling, and an additional factor of about 4 from wavefunction overlap suppression due to the very different scales involved. This reduces the relative rescattering contribution to $\omega\omega$ by almost an order of magnitude. An $f_0(1810)$ signal in this channel would not be observed by DM2, and at best marginally with the BES statistics.

As for the current absence of a BES $f_0(1810)$ signal in $K\bar{K}$, we submit that a more extensive measurement will observe this decay. This should include a careful examination of any enhancement in the tail of the established $f_0(1710) \rightarrow K\bar{K}$ decay. A related issue, first pointed out in [17, 18], is that the $\omega\phi \rightarrow K\bar{K}3\pi$ is a distinctive, novel glueball signature that is easily detected. It may be that the other decay channels were more difficult to observe due to pion background effects (e.g. $\rho\rho \rightarrow 4\pi$ and $\omega\omega \rightarrow 6\pi$ and even $\eta\eta, \eta\eta' \rightarrow$ multiple π).

Table 5. Rearrangement potential factors and ratio of widths for different channels using $V_{SS} \simeq 200$ MeV. See Appendix B for details

1 \rightarrow 2	$ \text{Spin} ^2$	$ \text{Flavor} ^2$	$ v_{\text{re}} $	Γ_2/Γ_1
$K^*\bar{K}^* \rightarrow \phi\omega$	25/4	2	100 MeV	0.044
$K\bar{K} \rightarrow \phi\omega$	3	2	69 MeV	0.006
$\rho\rho \rightarrow \omega\omega$	25/4	9/4	106 MeV	0.020
$\pi\pi \rightarrow \omega\omega$	3	9/4	73 MeV	0.011

4 Alternative $f_0(1810)$ scenarios

4.1 Threshold cusp

We first examine the possibility that a threshold cusp [29] explains the structure in the $\omega\phi$ spectrum. This kinematical enhancement occurs when a two-body system inelastically couples strongly to another open channel near threshold. Even at 1.8 GeV this condition is possible, and this would produce a low momentum scattering amplitude having the form $A + B/k$ with k the $\omega\phi$ center of mass momentum. However, multiplying the BES data by kinematical factors appropriate to each bin yields a resonance that is well separated from threshold, which seems to rule out this option.

Furthermore, the DM2 $\omega\omega$ and $\rho\rho$ data should have a similar cusp, but there are none. Rather, these data reveal a prominent peak, the $\eta(1760)$, 200 MeV above threshold, and clearly monotonically fall towards lower energies.

4.2 Conventional or hybrid meson

Even though there have been many scalar meson studies, their structure is still not completely understood. In the absence of mixing (claimed to be significant in most analyses), quark model f_0 states have 2 isoscalar flavor combinations, $s\bar{s}$ and $n\bar{n} = (u\bar{u} + d\bar{d})/\sqrt{2}$, with $^{2S+1}L_J = ^3P_0$. Their ground states are slightly above 1 GeV [30], and for this argument we use 1.1 and 1.4 GeV for the light and strange quark combinations, respectively. Adding 500–600 MeV for the required radial excitation (e.g. $\phi(1020)$ and its radial excitation $\phi(1680)$) yields 1.6–1.7 GeV for the light, and 2 GeV for the strange combination. The light quark combination is marginally too low while the $s\bar{s}$ radial excitation state is too high to explain a resonance at 1.8 GeV. Moreover, one would expect the latter to have a sizeable $K\bar{K}$ branching fraction, but this is not visible in the Mark III data [20], where the $f_0(1710)$ is dominant. Mixing the $f_0(1710)$ with a $n\bar{n}$ radial excitation may perhaps explain the BES peak. If so its decay to $f_0(1370)\pi\pi$ might be visible, however there is no simple mechanism explaining why this state should appear in J/ψ decays. Although this assignment cannot be rejected, these arguments make us suspicious.

We next examine hybrid mesons. In many body theory [31], hybrid mesons with the minimal Fock space assignment $q\bar{q}g$ in an s-wave yield a triplet $(0, 1, 2)^{++}$ and a pseudovector 1^{+-} . However, for typical values of the string tension, $\sqrt{\sigma} = 367$ MeV, their masses are near but above 2 GeV. Similar, though a bit lighter, results are obtained in the flux tube model and lattice gauge theory, so one cannot discard a hybrid state as low as 1.8 GeV. However, qualitatively comparing hybrid and glueball total width calculations, the hybrid width will be much broader, since there is only one gluon–quark vertex interaction, instead of two, yielding one less factor of α_s^2 suppression. Therefore a broader state than the BES result is expected.

4.3 The $f_0(1710)$ tail

The mass and width of the $f_0(1710)$, another glueball candidate, are poorly determined and the PDG values are $M = 1714(5)$ MeV, $\Gamma = 140(10)$ MeV. However, consistent with recent BES data, these values could be as high as $M = 1740$ MeV, $\Gamma = 166$ MeV. In this case, an overlap with the trailing edge of the $f_0(1710)$ Breit–Wigner distribution could produce the observed $\omega\phi$ signal. However, this possibility appears unlikely considering the near threshold behavior of the BES $\omega\phi$ spectrum. As in the cusp hypothesis, the current data seems to indicate that the resonance is separated from the threshold and therefore cannot stem from the $f_0(1710)$. Higher sample count studies would be very useful.

4.4 Four quark states

Tetraquark systems, another actively investigated area, also appear naturally as an intermediate step in a J/ψ decay chain. However, as in the hybrid case, one expects a four quark state to decay with a broad width generating a background, not a sharp signal, for radiative J/ψ decay. Related with this is that a realistic tetraquark width prediction also requires including $K\bar{K}$ rescattering effects, since the $\omega\phi$ attraction is not as strong as in $K\bar{K}$, where annihilation diagrams provide attractive forces. The quark rearrangement coupling between the $K^*\bar{K}^*$ and $\omega\phi$ channels also provides attraction (see Appendix B). This follows from the resonating group method (RGM) [32–34], which predicts an increased attraction between mesons when each has a quark and antiquark of the same flavor. Hence if the BES state is not a glueball, the RGM coupled channels will play an important role in elucidating its structure and applications of our model to this system are in progress.

5 Summary and conclusions

In this work we have examined and compared independent J/ψ decay data sets in the 1800 MeV mass region. Based on the data reported by the BES collaboration, we believe that the newly found $f_0(1810)$ is a promising glueball candidate or a state with a large glueball component. Significantly, its mass and quantum numbers are in agreement with previous theoretical expectations and its somewhat surprising narrow width of the order of 100 MeV is consistent with new fundamental calculations. We have addressed the perplexing issue of its selective decay to the $\omega\phi$ channel and discussed why it was not observed in both the BESII and the smaller sample DM2 measurements in the $\omega\omega$ channel. Also the $\pi\pi$ and $K\bar{K}$ channels have been examined by MARK III, and only the broad $f_0(1710)$ structure is apparent. However, the binning of these data is somewhat coarse and further structure cannot be ruled out. The DM2 data [35] shows a falling slope probably due to the $f_0(1710)$ tail. Higher precision studies are clearly needed.

We also noted that the rescattering process, $J/\psi \rightarrow \gamma G \rightarrow \gamma K \bar{K} \rightarrow \gamma \omega \phi$, may be producing the BES signal. In view of the importance of glueballs, we submit that a precision study of the $K \bar{K}$ spectrum is crucial for either resolving this or, more exciting, indeed establishing a new gluonic state near 1800 MeV.

Acknowledgements. F.J. Llanes-Estrada appreciates inspiring discussions on J/ψ decays with W.S. Hou and also on glueball widths with A. Goldhaber. Work supported in part by Spanish grants FPA 2004-02602, 2005-02327, PR27/05-13955-BSCH (FJL), U.S. DOE Grant No. DE-FG02-03ER41260 (SRC), Research Corporation (DGR) and the Ohio Supercomputer Center (DGR).

Appendix A: Computation of the inclusive decay width

Here we present the many body effective QCD Hamiltonian calculation for the glueball decay to four quarks that subsequently hadronize. In the Coulomb gauge the effective quark Hamiltonian contains an instantaneous interaction, mediated by the infrared enhanced Coulomb potential, and a transverse gluon exchange interaction that is infrared suppressed via the generation of a mass gap [36]. First the instantaneous interaction is diagonalized to obtain the glueball bound state wavefunction. Then the triple quark–gluon coupling interaction

$$H_{qg} = g \int d\mathbf{x} \bar{\Psi}^\dagger T^a \boldsymbol{\alpha} \Psi \cdot \mathbf{A}^a \quad (\text{A.1})$$

is treated perturbatively to compute the decay amplitude. Omitting the momentum conserving delta functions arising from the commutators, the integrand, I of the matrix element in (3) reduces to

$$\begin{aligned} I(G \rightarrow q_1 q_2 q_3 q_4) &= \text{CT} \sqrt{2} \frac{g^2(k)}{2\omega(k)} \sqrt{2M^2 E_1^2 E_2^2 E_3^2 E_4^2} \\ &\times \frac{\phi(k)}{\sqrt{4\pi}} G S c_1 c_2 c_3 c_4 (\hat{\mathbf{q}}_1 \hat{\mathbf{q}}_2 \hat{\mathbf{q}}_3 \hat{\mathbf{q}}_4). \end{aligned} \quad (\text{A.2})$$

For total (inclusive) decay the color tensor is

$$\text{CT} = \frac{\delta_{ab}}{\sqrt{8}} T_{c_1 c_2}^a T_{c_3 c_4}^b, \quad (\text{A.3})$$

which when squared and summed over the quark color indices C_i yields the squared color factor $\text{CF}^2 = 1/4$. The above result is for only one specific flavor and below we include the modification for application to three light flavors (u, d, s). The $\sqrt{2}$ factor is a result of gluon exchange symmetry and the glueball normalization in (4). The gluon self-energy, $\omega(k)$, follows from the intermediate gluon propagators in Fig. 3 and is the solution of a mass gap equation that is well approximated by $\sqrt{m_g^2 + k^2}$ (used here). The tensor S depends on the spinors in the Fourier expansion of

the quark field Ψ and the Dirac $\boldsymbol{\alpha}$ matrices coupled to the gluon spins. These spinors are usually expressed in terms of a BCS angle, whose relation to the running mass (from the quark gap equation) is $\sin \phi(q) = s_q = m(q)/\sqrt{m(q)^2 + q^2}$ (here we fix $m(q) = m$). Squaring the matrix element and summing over spins in the final state, we find, in terms of unit momentum vectors

$$\begin{aligned} \sum_{c_1 c_2 c_3 c_4} |S|^2 &= (1 + s_1 s_2)(1 + s_3 s_4) \\ &+ (1 + s_1 s_2) c_3 c_4 \hat{\mathbf{k}} \cdot \hat{\mathbf{q}}_3 \hat{\mathbf{k}} \cdot \hat{\mathbf{q}}_4 \\ &+ (1 + s_3 s_4) c_1 c_2 \hat{\mathbf{k}} \cdot \hat{\mathbf{q}}_1 \hat{\mathbf{k}} \cdot \hat{\mathbf{q}}_2 \\ &+ c_1 c_2 c_3 c_4 \left[\hat{\mathbf{q}}_1 \cdot \hat{\mathbf{q}}_3 \hat{\mathbf{q}}_2 \cdot \hat{\mathbf{q}}_4 + \hat{\mathbf{q}}_2 \cdot \hat{\mathbf{q}}_3 \hat{\mathbf{q}}_1 \cdot \hat{\mathbf{q}}_4 - \hat{\mathbf{q}}_1 \cdot \hat{\mathbf{q}}_2 \hat{\mathbf{q}}_3 \cdot \hat{\mathbf{q}}_4 \right. \\ &- \hat{\mathbf{k}} \cdot \hat{\mathbf{q}}_2 \hat{\mathbf{k}} \cdot \hat{\mathbf{q}}_4 \hat{\mathbf{q}}_1 \cdot \hat{\mathbf{q}}_3 - \hat{\mathbf{k}} \cdot \hat{\mathbf{q}}_1 \hat{\mathbf{k}} \cdot \hat{\mathbf{q}}_4 \hat{\mathbf{q}}_2 \cdot \hat{\mathbf{q}}_3 + \hat{\mathbf{k}} \cdot \hat{\mathbf{q}}_1 \hat{\mathbf{k}} \cdot \hat{\mathbf{q}}_2 \hat{\mathbf{q}}_3 \cdot \hat{\mathbf{q}}_4 \\ &+ \hat{\mathbf{k}} \cdot \hat{\mathbf{q}}_3 \hat{\mathbf{k}} \cdot \hat{\mathbf{q}}_4 \hat{\mathbf{q}}_1 \cdot \hat{\mathbf{q}}_2 - \hat{\mathbf{k}} \cdot \hat{\mathbf{q}}_2 \hat{\mathbf{k}} \cdot \hat{\mathbf{q}}_3 \hat{\mathbf{q}}_1 \cdot \hat{\mathbf{q}}_4 - \hat{\mathbf{k}} \cdot \hat{\mathbf{q}}_1 \hat{\mathbf{k}} \cdot \hat{\mathbf{q}}_3 \hat{\mathbf{q}}_2 \cdot \hat{\mathbf{q}}_4 \\ &\left. + 2\hat{\mathbf{k}} \cdot \hat{\mathbf{q}}_1 \hat{\mathbf{k}} \cdot \hat{\mathbf{q}}_2 \hat{\mathbf{k}} \cdot \hat{\mathbf{q}}_3 \hat{\mathbf{k}} \cdot \hat{\mathbf{q}}_4 \right]. \end{aligned} \quad (\text{A.4})$$

Since all possible relative angles in the final state appear, I is only invariant under rigid rotations of the five vectors. With this, the squared decay matrix element summed over the final state color, spin and flavor indices reads

$$\begin{aligned} \sum |I|^2 &= \text{FF}^2 R \\ R &= \text{CF}^2 \frac{2}{4\omega(k)^2} 2M^2 E_1^2 E_2^2 E_3^2 E_4^2 \\ &\times \frac{|\phi(k)|^2}{4\pi} (4\pi \alpha_s(k))^2 |G S_{1234}|^2. \end{aligned} \quad (\text{A.5})$$

Symmetry considerations apply if both emitted quark–antiquark pairs are indistinguishable and we absorb this into the flavor factor FF^2 below.

Let us now examine the phase space integrals. Momentum conservation for a decaying glueball at rest requires

$$\mathbf{q}_1 + \mathbf{q}_2 + \mathbf{q}_3 + \mathbf{q}_4 = 0, \quad (\text{A.6})$$

yielding for the gluon momentum

$$\mathbf{k} = \mathbf{q}_1 + \mathbf{q}_2 = -\mathbf{q}_3 - \mathbf{q}_4. \quad (\text{A.7})$$

There are nine integration variables in (8). We can arbitrarily fix \mathbf{k} along the third axis and obtain a 4π factor for global rotations. Further we can integrate one azimuthal angle (say ϕ_1) around this fixed axis, an operation preserving all relative angles. The modulus $k = |\mathbf{k}|$ remains an independent variable. The others can be chosen as $q_1 = |\mathbf{q}_1|$, $\cos \theta_{q_1 k}$ (which automatically fixes \mathbf{q}_1 and \mathbf{q}_2), and the three spherical coordinates of \mathbf{q}_3 , $q_3 = |\mathbf{q}_3|$, $\cos \theta_{q_3 k}$ and ϕ_3 . Only five of these six are independent, since we have not utilized the energy conservation relation. This imposes cumbersome restrictions on the angular variables, so it is convenient and customary to introduce an auxiliary variable, \mathcal{E} , representing the energy of the second pair, by means of

$$\begin{aligned} \delta \left(M_G - \sum E_i \right) &= \int \delta(M_G - \mathcal{E} - E_1 - E_2) \\ &\times \delta(\mathcal{E} - E_3 - E_4) d\mathcal{E}. \end{aligned} \quad (\text{A.8})$$

The two δ functions can be used to integrate over the two polar angles $\cos\theta_{q_1k}$ and $\cos\theta_{q_3k}$, leaving only the \mathcal{E} integration with integration limits fixed by the requirement that the cosine values remain in the interval $(-1, 1)$. This is easily implemented in our 5 dimensional Monte Carlo computation by rejecting points exceeding this bound. The resulting polar cosines are

$$\cos\theta_{q_1k} = \frac{m_2^2 + q_1^2 + k^2 - (M_G - \mathcal{E} + E_1)^2}{2kq_1}, \quad (\text{A.9})$$

$$\cos\theta_{q_3k} = \frac{(\mathcal{E} - E_3)^2 - (m_4^2 + q_3^2 + k^2)}{2kq_3}. \quad (\text{A.10})$$

Note that the change of variable from energy to angle in each of the δ functions adds an extra factor

$$\begin{aligned} \delta(E_0 - E) &= \delta(E_0 - \sqrt{m^2 + k^2 + q^2 + 2kq \cos\theta}) \\ &= \frac{E_0}{kq} \delta(\cos\theta_0 - \cos\theta). \end{aligned} \quad (\text{A.11})$$

There are then four remaining integration variables k , q_1 , q_3 , ϕ_3 , for a total of five integrals that are performed numerically. A representation for the coupling α_s in the infrared is needed and we use [37]

$$\alpha_s(k) = \frac{4\pi}{9 \log((k^2 + M_0^2)/\Lambda^2)}, \quad (\text{A.12})$$

with $\Lambda \simeq 0.2\text{--}0.21$ GeV and $M_0 \simeq 1\text{--}1.1$ GeV. The final ingredient is the propagator $g(\mathbf{x}, \mathbf{y})$ for the intermediate hybrid meson cut in Fig. 3, necessary for a second order calculation. Its exact energy eigenfunction expansion is

$$g = \sum_{h=\text{hybrid}} |h\rangle \frac{1}{M_G - E_h - i\epsilon} \langle h|. \quad (\text{A.13})$$

The spectrum of hybrid mesons has been studied with this many body method in [31] where, for string tension $\sqrt{\sigma} = 367$ MeV, the ground state scalar hybrid meson has mass 2100 MeV. Excitations thereof appear with spacings similar to those in ordinary meson quark models. We use $g = 1/(M_G - M_h) \simeq 1/(300 \text{ MeV})$ and dressed quark masses $m_u = m_d = 100$ MeV, $m_s = 200$ MeV, consistent with prior work using the same approach and parameters. These values are typical of the masses calculated in [38], but somewhat low compared to quark model phenomenology, since in field theory approaches a sizeable fraction of the hadron mass originates in the self-energy contribution in the bound state problem and not in the mass gap equation. These values also yield a realistic conventional hadron spectrum. Similarly we have $m_g = \omega(0) = 650$ MeV, where $\omega(k)$ is the solution of the gluon gap equation of pure gluodynamics [6].

Finally, let us examine the flavor factors. For an inclusive decay we can separate the sum over the final states

$$\sum_{\text{flavor}} |I|^2 = \sum_{\text{diff}} |I|^2 + \sum_{\text{same}} |I|^2 = \text{FF}^2 R, \quad (\text{A.14})$$

where

$$\begin{aligned} \text{FF} &\propto \langle \Omega | (u\bar{u} + d\bar{d} + s\bar{s}) \sum_{q'\bar{q}'} |q'\bar{q}'\rangle \\ &\quad \langle q'\bar{q}' | (u\bar{u} + d\bar{d} + s\bar{s}) | q\bar{q}q\bar{q} \rangle. \end{aligned} \quad (\text{A.15})$$

We have

$$\text{FF}^2 = 4 \cdot 3 + \frac{1}{2^2} \cdot 16 \cdot 3 = 24, \quad (\text{A.16})$$

where the first term accounts for the case where the outgoing quark pairs have different flavors, and the second for the case where the outgoing flavors are the same. The 3 in each term reflects the number of distinct choices for three flavors (u, d, s), and the $1/2^2$ corrects for over-counting in the sum over final states with two pairs of identical particles. If we separate by flavor channel the corresponding factors are 12 for light–light, 8 for light–strange and 4 for strange–strange. With this we obtain the complete expression for the glueball width (see Table 4 for numerical results)

$$\begin{aligned} \Gamma &= \frac{(2\pi)(4\pi)}{(2\pi)^9} \int_0^{M_G} 2\pi d\mathcal{E} \int_0^{2\pi} d\phi_3 \int_0^{M_G/2} k^2 dk \\ &\quad \times \int_0^{M_G/2} q_1^2 dq_1 \int_0^{M_G/2} q_3^2 dq_3 \\ &\quad \times \frac{E_2}{kq_3} \frac{E_4}{kq_1} \frac{1}{(M_G - M_h)^2} \text{CF}^2 \text{FF}^2 \frac{2}{4\omega_k^2} \frac{|\phi(k)|^2}{4\pi} |S|^2 \\ &\quad \times (4\pi\alpha_s(k))^2 \Theta(\cos^2\theta_{q_1k} - 1) \Theta(\cos^2\theta_{q_3k} - 1). \end{aligned} \quad (\text{A.17})$$

Appendix B: Resonating group method and decay channel recoupling

In this appendix we theoretically treat the sequential decay of a glueball G to a meson pair followed by rearrangement. To be specific, we assume that G first decays to $K^* \bar{K}^*$ and then to $\phi\omega$, as depicted in Fig. 4.

B.1 Coupled channels

We approximately solve the equation of motion, $H\Phi = E\Phi$, using the resonating group/coupled channels formalism [32–34] for this three channel problem

$$\begin{aligned} &\begin{pmatrix} H_G - E - i\epsilon & V_{\text{sb}} & 0 \\ V_{\text{sb}}^* & H_{K^* \bar{K}^*} - E - i\epsilon & V_{\text{re}} \\ 0 & V_{\text{re}}^* & H_{\phi\omega} - E - i\epsilon \end{pmatrix} \\ &\times \begin{pmatrix} \Phi_G \\ \Phi_{K^* \bar{K}^*} \\ \Phi_{\phi\omega} \end{pmatrix} = 0, \end{aligned} \quad (\text{B.1})$$

where V_{sb} is the string breaking decay coupling between the glueball and the open flavor channel, and V_{re} is the rearrangement potential, coupling the latter to the $\phi\omega$ channel. We now extract the glueball width Γ from the imaginary part of the resulting glueball energy/mass. Since $H_G \simeq M_G = 1812 \text{ MeV}$ and from our computation of the total glueball width, it follows that V_{sb} is at most of order 100 MeV. We can therefore diagonalize using perturbation theory to the leading order in V_{sb} ,

$$\left[H_G - E - V_{\text{sb}} \left(\frac{1}{H_{K^*\bar{K}^*} - E - i\epsilon} + \frac{1}{H_{K^*\bar{K}^*} - E - i\epsilon} V_{\text{re}} \frac{1}{H_{\phi\omega} - E - i\epsilon} \times V_{\text{re}}^* \frac{1}{H_{K^*\bar{K}^*} - E - i\epsilon} + \dots \right) V_{\text{sb}}^* \right] \Phi_G = 0, \quad (B.2)$$

$$\left(H_{\text{eff}}(E) - \frac{i}{2} \Gamma(E) - E \right) \Phi_G = 0.$$

Also using perturbation theory for V_{re} , we identify the imaginary part of the first potential term, to order V_{sb}^2 , as the partial decay width to $K^*\bar{K}^*$, while the contribution (for an open $\phi\omega$ channel) to the imaginary part from the second term, to order $V_{\text{sb}}^2 V_{\text{re}}^2$, yields the partial decay width for $\phi\omega$. The same analysis can be used for other sequential decays, e.g. $G \rightarrow \pi\pi \rightarrow \omega\omega$.

In evaluating the string breaking and rearrangement potentials, we truncate the sum over intermediate hadron states to the ground state mesons in each channel c and employ harmonic oscillator wavefunctions, $\phi_0^{\alpha c}$, having oscillator parameter α_c . This yields the following separable potentials for string breaking:

$$V_{\text{sb}} = v_{\text{sb}} |\phi_0^{\alpha c}\rangle \langle \phi_0^{\alpha c}|, \quad (B.3)$$

and rearrangement,

$$V_{\text{re}} = v_{\text{re}} |\phi_0^{\alpha c}\rangle \langle \phi_0^{\alpha c}|, \quad (B.4)$$

and the resulting partial widths,

$$\begin{aligned} \Gamma_{K^*\bar{K}^*} &= 2|v_{\text{sb}}|^2 \text{Im} [g_{K^*\bar{K}^*}(E)], \\ \Gamma_{\phi\omega} &= 2|v_{\text{sb}}|^2 |v_{\text{re}}|^2 \text{Re} [g_{K^*\bar{K}^*}(E)] \\ &\quad \times \text{Im} [g_{\phi\omega}(E)] \text{Re} [g_{K^*\bar{K}^*}(E)], \\ g_c(E) &= \langle \phi_0^{\alpha c} | \frac{1}{M_c + \frac{g^2}{2\mu_c} - E - i\epsilon} | \phi_0^{\alpha c} \rangle. \end{aligned} \quad (B.5)$$

Here M_c and μ_c are the threshold energy and reduced mass for channel c . Because the glueball mass is near the channel thresholds, the real and imaginary parts of the channel Green functions, $g_c(E) = a_c + ib_c$, can be well approximated by

$$a_c \simeq \frac{\int_0^\infty \frac{e^{-\alpha_c^2 q^2}}{g^2} q^2 dq}{\int_0^\infty e^{-\alpha_c^2 q^2} q^2 dq} = 4\alpha_c^2 \mu_c, \quad (B.6)$$

$$b_c \simeq 4\alpha_c^3 \mu_c \sqrt{2\pi\mu_c} \sqrt{E - M_c}, \quad (B.7)$$

Table 6. Rescattering parameters

$c \rightarrow$	$\phi\omega$	$\omega\omega$	$K^*\bar{K}^*$	$\rho\rho$	$K\bar{K}$	$\pi\pi$
$10^3 a_c (\text{MeV}^{-1})$	2.74	2.41	2.75	2.38	2.16	1.18
$10^3 b_c (\text{MeV}^{-1})$	0.57	2.35	0.96	2.40	3.51	1.20
$\alpha_c^{-1} (\text{MeV})$	804	804	804	804	603	483
$\mu_c (\text{MeV})$	443	391	446	385	248	69
$M_c (\text{MeV})$	1802	1564	1784	1540	994	278

and $E = M_G$. The partial decay widths are then

$$\begin{aligned} \Gamma_{K^*\bar{K}^*} &= 2|v_{\text{sb}}|^2 b_{K^*\bar{K}^*}, \\ \Gamma_{\phi\omega} &= 2|v_{\text{sb}}|^2 |v_{\text{re}}|^2 a_{K^*\bar{K}^*}^2 b_{\phi\omega}. \end{aligned} \quad (B.8)$$

The only model dependent quantities are the potential strengths v_{re} and v_{sb} , but only one enters the ratio of the two partial decay widths. Because the vector mesons have the same oscillator parameter and the reduced masses μ_c are similar, while the thresholds M_c differ for $K^*\bar{K}^*$ and $\phi\omega$, the ratio reduces to

$$\frac{\Gamma_{\phi\omega}}{\Gamma_{K^*\bar{K}^*}} = (v_{\text{re}} 4\mu_{\phi\omega} \alpha_{\phi\omega}^2)^2 \sqrt{\frac{M_G - M_{\phi\omega}}{M_G - M_{K^*\bar{K}^*}}}. \quad (B.9)$$

The parameters used in our calculation are listed in Table 6. Notice that we did not compute the complete geometric series in (B.2). If the ratio, (B.9), is large, we need to sum the full geometric series in (B.2). However, the remaining terms of the series contribute the same factor for the decay to $K^*\bar{K}^*$, or to $\phi\omega$, and therefore the ratio is correct to all orders in V_{re} .

B.2 String breaking

Because the ratio in (B.9) simplifies, we only list the flavors directly produced with string breaking. Notice that the same flavors are produced with a direct decay of the constituent gluons. Let us suppose that there are two string breakings producing two mesons. We assume that each string breaking creates a quark–antiquark pair in an approximately symmetric way, yielding an SU(3) flavor singlet

$$u\bar{u} + d\bar{d} + s\bar{s}, \quad (B.10)$$

where we suppress spin and color notation. In the string breaking picture, the quarks will be separated, each to one of the two produced mesons. This is also necessary to ensure that each of the produced mesons is a color singlet (equivalent to having quark exchange between the two flavor singlet sources and the two produced mesons). Exchanging the first and third quarks (permutation operator P^{13}) yields

$$\begin{aligned} P^{13} |(u\bar{u} + d\bar{d} + s\bar{s})(u\bar{u} + d\bar{d} + s\bar{s})| \\ = |u\bar{u}u\bar{u} + d\bar{d}d\bar{d} + u\bar{d}d\bar{u} + d\bar{u}u\bar{d} \\ + u\bar{s}s\bar{u} + s\bar{u}u\bar{s} + d\bar{s}s\bar{d} + s\bar{d}d\bar{s} + s\bar{s}s\bar{s})| \end{aligned}$$

$$= \left| \frac{u\bar{u} + d\bar{d}}{\sqrt{2}} \frac{u\bar{u} + d\bar{d}}{\sqrt{2}} + \frac{u\bar{u} - d\bar{d}}{\sqrt{2}} \frac{u\bar{u} - d\bar{d}}{\sqrt{2}} \right. \\ \left. + u\bar{d}\bar{d} + d\bar{u}\bar{u} + u\bar{s}\bar{s} + s\bar{u}\bar{u} + d\bar{s}\bar{s} + s\bar{d}\bar{d} + s\bar{s}\bar{s} \right\rangle, \quad (\text{B.11})$$

with a similar result for the exchange of the second and fourth antiquarks (P^{24}).

Specializing to vector–vector production, nine different vector pairs are produced and (B.11) becomes

$$= |\omega\phi + \rho^0\rho^0 + \rho^+\rho^- + \rho^-\rho^+ \\ + K^{*+}K^{*-} + K^{*-}K^{*+} + K^{*0}\bar{K}^{*0} + \bar{K}^{*0}K^{*0} + \phi\phi\rangle, \quad (\text{B.12})$$

but no $\omega\phi$ from string breaking. This explains why the off-diagonal Hamiltonian matrix element coupling this channel in (B.1) is zero and that $\omega\phi$ can only be produced by rearrangement.

B.3 Rearrangement

In evaluating $\Gamma_{\phi\omega}$ for the partial width ratio, (B.9), the normalized $|K^*\bar{K}^*\rangle$ and $|\omega\phi\rangle$ states are needed. The $\omega\phi$ component is

$$|\omega\phi\rangle = \left| \frac{u\bar{u} + d\bar{d}}{\sqrt{2}} s\bar{s} \right\rangle, \quad (\text{B.13})$$

while $K^*\bar{K}^*$ is given by

$$|K^*\bar{K}^*\rangle = \left| \frac{K^{*+}K^{*-} + K^{*-}K^{*+} + K^{*0}\bar{K}^{*0} + \bar{K}^{*0}K^{*0}}{\sqrt{2}\sqrt{4}} \right\rangle \\ = \left| \frac{u\bar{d}\bar{d} + d\bar{u}\bar{u} + u\bar{s}\bar{s} + s\bar{u}\bar{u}}{\sqrt{2}\sqrt{4}} \right\rangle, \quad (\text{B.14})$$

where the wavefunction normalization includes the meson–meson exchange,

$$\langle K^*\bar{K}^* | 1 + P^{13}P^{24} | K^*\bar{K}^* \rangle = 1. \quad (\text{B.15})$$

Then the flavor rearrangement matrix element involving P^{13} quark–quark exchange is

$$\langle K^{*+}K^{*-} | P^{13} | \phi\omega \rangle = \frac{1}{2}. \quad (\text{B.16})$$

Notice that P^{24} antiquark–antiquark exchange produces exactly the same result. This also applies to the color and spin \times space rearrangement overlaps, so we only compute the P^{13} overlaps and include an additional factor of 2 to account for antiquark exchange.

The color rearrangement overlap is

$$\langle 11 | P^{13} | 11 \rangle = \frac{1}{3}. \quad (\text{B.17})$$

For the space \times spin matrix element, using the graphical rules [39, 40], a separable potential with strength v emerges,

$$\langle \phi_0^\alpha \phi_0^\alpha | P^{13} | \phi_0^\alpha \phi_0^\alpha \rangle = v |\phi_0^\alpha\rangle \langle \phi_0^\alpha|. \quad (\text{B.18})$$

Hence, only the hyperfine interaction,

$$V_{SS} \frac{\lambda_i \cdot \lambda_j}{-16/3} \mathbf{S}_i \cdot \mathbf{S}_j \quad (\text{B.19})$$

contributes to the space \times spin rearrangement, and the potential v is proportional to $V_{SS} \simeq 200$ MeV, obtained from [41]. To determine this constant we consider the specific overlap where both $K^*\bar{K}^*$ and $\phi\omega$ have a total spin 0. Coupling two vector mesons yields

$$|00\rangle = \frac{|11\rangle|1-1\rangle - |10\rangle|10\rangle + |1-1\rangle|11\rangle}{\sqrt{3}} \\ = \left| \frac{\uparrow\uparrow\downarrow\downarrow + \downarrow\downarrow\uparrow\uparrow}{\sqrt{3}} - \frac{\uparrow\downarrow\uparrow\downarrow + \uparrow\downarrow\downarrow\uparrow + \downarrow\uparrow\uparrow\downarrow + \downarrow\uparrow\downarrow\uparrow}{2\sqrt{3}} \right\rangle, \quad (\text{B.20})$$

so that

$$\langle 00 | P^{13} | 00 \rangle_{VV \rightarrow VV} = -\frac{1}{2}. \quad (\text{B.21})$$

An analogous calculation shows the recoupling of two pseudoscalars to give two pseudoscalars or two pseudoscalars to two vectors,

$$\langle 00 | P^{13} | 00 \rangle_{PP \rightarrow PP} = \frac{1}{2}, \\ \langle 00 | P^{13} | 00 \rangle_{PP \rightarrow VV} = -\frac{\sqrt{3}}{2}. \quad (\text{B.22})$$

Only the intra-cluster contributions $V_{13}, V_{14}, V_{23}, V_{24}$ of the hyperfine potential need to be considered [42, 43], since the intercluster ones are already included in the meson mass calculation. Adding all intracluster contributions, the total space \times spin overlap contribution for this case is

$$-\frac{3}{2} V_{SS} |\phi_0^\alpha\rangle \langle \phi_0^\alpha|. \quad (\text{B.23})$$

Then the resulting color \times flavor \times space \times spin overlap contribution for this case is

$$-\frac{1}{2} V_{SS} |\phi_0^\alpha\rangle \langle \phi_0^\alpha|, \quad (\text{B.24})$$

yielding the strength and sign for the rearrangement potential

$$v_{re} = -\frac{1}{2} V_{SS}. \quad (\text{B.25})$$

The value of α is fixed by the rms radius, $\langle r^2 \rangle$, of the corresponding meson. For a Gaussian wavefunction

$$\langle r^2 \rangle = \frac{\int_0^\infty dr r^4 e^{-r^2/\alpha^2}}{\int_0^\infty dr r^2 e^{-r^2/\alpha^2}} \\ = \frac{3}{2} \alpha^2. \quad (\text{B.26})$$

For the pion $\langle r^2 \rangle^{1/2} \simeq 0.5$ fm, but this is anomalously large due to the light mass (in chiral perturbation theory it is divergent in the chiral limit). We use 0.4 fm for

kaons and 0.3 fm for all vector mesons. Converting to MeV^{-1} , Table 6 lists the oscillator parameters used for each channel.

B.4 Mixing with conventional $q\bar{q}$ mesons

The issue of mixing between conventional $q\bar{q}$ mesons and glueballs, which certain studies [9, 10] have investigated, needs to be addressed; especially possible effects on calculated glueball widths from decays via quark wavefunction components. Here we argue, in the context of the Coulomb gauge quantum chromodynamics that inspires our model, that mixing is not a dominant mechanism but rather a correction to our study at the wavefunction level. We are currently performing a large-scale, detailed mixing investigation within our field theory approach that includes both quark and gluon Fock sectors without additional parameters and will report completed results in a future publication [44]. Here we present a simple mixing estimate.

Consider Fig. 5, which illustrates the most logical mechanism for a gg glueball to decay via quark mixing. This three step process entails $g \rightarrow q\bar{q}$ production (step 1) followed by an intermediate hybrid meson proceeding to a conventional meson (step 2), which then connects to a $q\bar{q}q\bar{q}$ two meson final state (step 3). The argument why conventional meson mixing should not change the width estimate substantially now follows.

In our model the final step (between steps 2 and 3, $q\bar{q} \rightarrow q\bar{q}q\bar{q}$) involves two types of suppression depending upon intermediate meson state. The first type involves the ground state $u\bar{u}$ and $s\bar{s}$ mesons, which, using the same approach [30], are at 900 and 1250 MeV, far from the 1810 under discussion. The nearest conventional intermediate scalar meson state must therefore have 1 or more radial excitations, which (by the Sturm–Liouville theorem) have a node in their wavefunction producing significant wavefunction overlap cancellation. The second type of suppression is via large energy denominators (from perturbation theory) involving the remaining meson intermediate states having masses farther away from the 1.7 GeV unmixed glueball. Finally, the first two steps are governed entirely by the H_{gg} term of (A.1) and are thus much weaker, consistent with perturbation theory. The overall resulting multi-step transition probability will therefore be suppressed.

We now examine and discuss previous conventional mixing schemes. Application of their use in scalar meson radiative decays can be found, for example, in [45]. Con-

sider first the work by Lee and Weingarten [46], who performed a lattice computation yielding

$$\begin{pmatrix} f_0(1710) \\ f_0(1500) \\ f_0(1370) \end{pmatrix} = \begin{pmatrix} 0.86(5) & 0.30(5) & 0.41(9) \\ -0.13(5) & 0.91(4) & -0.40(11) \\ -0.50(12) & 0.29(9) & 0.82(9) \end{pmatrix} \begin{pmatrix} gg \\ s\bar{s} \\ n\bar{n} \end{pmatrix} \quad (\text{B.27})$$

in conventional notation. It is very surprising that a state such as the $f_0(1500)$, with a branching fraction to $K\bar{K}$ that is about about 9% (or a partial width of only 11 MeV) by current data, will be mostly composed of an $s\bar{s}$ conventional wavefunction. Also surprising is: why should the $f_1(1420)$, which appears to be an excellent candidate for the 3P_1 $s\bar{s}$ state, be lighter than the corresponding 3P_0 $s\bar{s}$, presumably near 1500 MeV, when established spin–orbit effects in charmonium yield the 3P_1 to be higher than the 3P_0 ?

Contrasting this, the phenomenological mixing analysis of Close and Kirk [47] yields a glueball mixed strongly among the three known scalar states,

$$\begin{pmatrix} f_0(1710) \\ f_0(1500) \\ f_0(1370) \end{pmatrix} = \begin{pmatrix} 0.39(3) & 0.91(2) & 0.15(2) \\ -0.65(4) & 0.33(4) & -0.70(7) \\ -0.69(7) & 0.15(1) & 0.70(7) \end{pmatrix} \begin{pmatrix} gg \\ s\bar{s} \\ n\bar{n} \end{pmatrix}. \quad (\text{B.28})$$

While this mixture is able to explain the broad features of the branching fractions for the three states, it is at odds with theory by requiring a surprising gg “bare” (or unmixed) glueball mass smaller than the conventional $s\bar{s}$ scalar meson, that is, below about 1450 MeV.

Therefore, the finding of a new state by the BES collaboration near 1800 MeV is indeed welcomed as it may ultimately resolve these issues.

We conclude with an estimate of the effect from mixing two quarkonium components with a “bare” $G = gg$ glueball of mass 1810 MeV. Consider the two kaon decay mode of a mixed state. To understand the “bare” states we utilize the $f_1(1420)$, with a predominantly 50 MeV width to $K\bar{K}^*$. Correcting only for spin counting and phase space in the final state we find again a width of $\Gamma_{s\bar{s} \rightarrow K\bar{K}} = 50$ MeV for the scalar decay. Presumably the $n\bar{n}$ coupling to the kaon channel is about half of the corresponding coupling of the $s\bar{s}$. We then combine this result with a mixed coupling constant for the 1810 given by the first mixing matrix above (top row), $g_{f_0} = 0.86g_G + 0.30g_{s\bar{s}} + 0.41g_{n\bar{n}}$. This yields an estimate for a mixed $f_0(1810)$ decay to $K\bar{K}$ and the widths in Table 4 increase from 15 to 46 MeV (first column) and 60 to 100 MeV (second column). If there is destructive mixing interference the effect will be less. We note that the mixing correction is a modest increase (shift) in the widths by about 30 to 40 MeV as opposed to a percentage increase since we have also performed “toy” calculations with an artificially enhanced “bare” width and find again the same 30 to 40 MeV increase from mixing. Assuming a conservative constructive mixing scenario, with phases given by various analyses, it appears that this mixing is likely to increase the predicted bare glueball width but not dramatically.

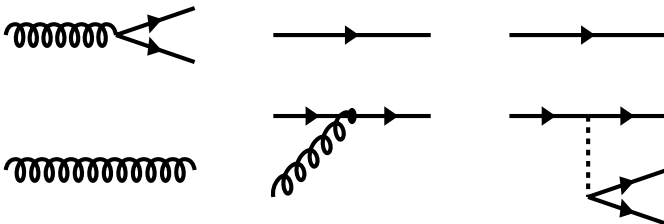


Fig. 5. Steps necessary for a glueball to decay into a $q\bar{q}q\bar{q}$ state by an intermediate conventional meson state

References

1. BES Collaboration, M. Ablikim, et al., Phys. Rev. Lett. **96**, 162002 (2006) [arXiv:hep-ex/0602031]
2. J.R. Pelaez, G. Rios, Phys. Rev. Lett. **97**, 242002 (2006) [arXiv:hep-ph/0610397]
3. Y.A. Simonov, Phys. Lett. B **249**, 514 (1990)
4. F.J. Llanes-Estrada, S.R. Cotanch, P. Bicudo, J.E. Ribeiro, A.P. Szczepaniak, Nucl. Phys. A **710**, 45 (2002) [arXiv:hep-ph/0008212]
5. C.J. Morningstar, M.J. Peardon, Phys. Rev. D **60**, 034509 (1999) [arXiv:hep-lat/9901004]
6. A. Szczepaniak, E.S. Swanson, C.R. Ji, S.R. Cotanch, Phys. Rev. Lett. **76**, 2011 (1996) [arXiv:hep-ph/9511422]
7. UKQCD Collaboration, A. Hart, C. McNeile, C. Michael, J. Pickavance, Phys. Rev. D **74**, 114504 (2006) [arXiv:hep-lat/0608026]
8. G. Bali et al., Phys. Lett. B **309**, 378 (1993)
9. F. Giacosa, T. Gutsche, V.E. Lyubovitskij, A. Faessler, Phys. Rev. D **72**, 094006 (2005) [arXiv:hep-ph/0509247]
10. V.V. Anisovich, AIP Conf. Proc. **619**, 197 (2002) [arXiv:hep-ph/0110326]
11. P. Minkowski, W. Ochs, Eur. Phys. J. C **9**, 283 (1999)
12. C. Amsler, F.E. Close, Phys. Lett. B **353**, 385 (1995) [arXiv:hep-ph/9505219]
13. D.V. Bugg, Phys. Rep. **397**, 257 (2004) [arXiv:hep-ex/0412045]
14. M. Chanowitz, Phys. Rev. Lett. **95**, 172001 (2005) [arXiv:hep-ph/0506125]
15. DM2 Collaboration, D. Bisello et al., Phys. Lett. B **192**, 239 (1987)
16. MARK-III Collaboration, R.M. Baltrusaitis et al., Phys. Rev. D **33**, 1222 (1986)
17. S.R. Cotanch, R.A. Williams, Phys. Rev. C **70**, 055201 (2004) [arXiv:nucl-th/0403051]
18. S.R. Cotanch, R.A. Williams, Phys. Lett. B **621**, 269 (2005) [arXiv:nucl-th/0505074]
19. BES Collaboration, M. Ablikim et al., arXiv:hep-ex/0604045
20. MARK-III Collaboration, W. Dunwoodie, AIP Conf. Proc. **432**, 753 (1998)
21. BES Collaboration, J.Z. Bai et al., Phys. Lett. B **472**, 200 (2000) [arXiv:hep-ex/9908045]
22. Particle Data Group, S. Eidelman et al., Phys. Lett. B **592**, 1 (2004)
23. J. Sexton, A. Vaccarino, D. Weingarten, Phys. Rev. Lett. **75**, 4563 (1995) [arXiv:hep-lat/9510022]
24. L. Burakovsky, P.R. Page, Phys. Rev. D **59**, 014022 (1999)
25. L. Burakovsky, P.R. Page, Phys. Rev. D [Erratum] **59**, 079902 (1999) [arXiv:hep-ph/9807400]
26. E. Abreu, P. Bicudo, arXiv:hep-ph/0508281
27. F.J. Llanes-Estrada, P. Bicudo, S.R. Cotanch, Phys. Rev. Lett. **96**, 081601 (2006) [arXiv:hep-ph/0507205]
28. C.E. Carlson, J.J. Coyne, P.M. Fishbane, F. Gross, S. Meshkov, Phys. Rev. D **23**, 2765 (1981)
29. D.V. Bugg, Phys. Lett. B **598**, 8 (2004) [arXiv:hep-ph/0406293]
30. F.J. Llanes-Estrada, S.R. Cotanch, Nucl. Phys. A **697**, 303 (2002) [arXiv:hep-ph/0101078]
31. F.J. Llanes-Estrada, S.R. Cotanch, Phys. Lett. B **504**, 15 (2001) [arXiv:hep-ph/0008337]
32. S.R. Cotanch, C.M. Vincent, Phys. Rev. C **14**, 1739 (1976) and references therein
33. P. Bicudo, S. Cotanch, F. Llanes-Estrada, P. Maris, E. Ribeiro, A. Szczepaniak, Phys. Rev. D **65**, 076008 (2002) [arXiv:hep-ph/0112015].
34. P. Bicudo, G.M. Marques, Phys. Rev. D **69**, 011503 (2004) [arXiv:hep-ph/0308073]
35. DM2 Collaboration, J.E. Augustin et al., Phys. Rev. Lett. **60**, 2238 (1988)
36. A.P. Szczepaniak, Phys. Rev. D **69**, 074031 (2004) [arXiv:hep-ph/0306030]
37. S.J. Brodsky, T. Huang, G.P. Lepage, 9th SLAC Summer Inst. on Particle Physics (1981)
38. F.J. Llanes-Estrada, S.R. Cotanch, A.P. Szczepaniak, E.S. Swanson, Phys. Rev. C **70**, 035202 (2004) [arXiv:hep-ph/0402253]
39. J.E. Ribeiro, Phys. Rev. D **25**, 2406 (1982)
40. E. van Beveren, Z. Phys. C **17**, 135 (1983)
41. P. Bicudo, J.E. Ribeiro, J. Rodrigues, Phys. Rev. C **52**, 2144 (1995)
42. P. Bicudo, J.E. Ribeiro, Phys. Rev. D **42**, 1635 (1990)
43. P. Bicudo, Phys. Rev. C **60**, 035209 (1999)
44. I.J. General, P. Wang, S.R. Cotanch, F.J. Llanes-Estrada, arXiv:0707.1286
45. M.A. DeWitt, H.M. Choi, C.R. Ji, Phys. Rev. D **68**, 054026 (2003) [arXiv:hep-ph/0306060]
46. W.J. Lee, D. Weingarten, Phys. Rev. D **61**, 014015 (2000) [arXiv:hep-lat/9910008]
47. F.E. Close, A. Kirk, Eur. Phys. J. C **21**, 531 (2001) [arXiv:hep-ph/0103173]